Japanese Journal of Applied Physics
Vol. 45, No. 3B, 2006, pp. 1992–1995

©2006 The Japan Society of Applied Physics

Scanning Probe with Tuning Fork Sensor, Microfabricated Silicon Cantilever and Conductive Tip for Microscopy at Cryogenic Temperature

Terunobu AKIYAMA, Kaspar SUTER, Nicolaas F. DE ROOIJ, Andreas BAUMGARTNER[1], Arnd E. GILDEMEISTER[1], Thomas IHN[1], Klaus ENSSLIN[1] and Urs STAUFER

Institute of Microtechnology, University of Neuchâtel, Jaquet-Droz 1, 2002 Neuchâtel, Switzerland
[1]*Nano-Physics Group, Laboratory of Solid State Physics, ETH Hönggerberg, 8093 Zürich, Switzerland*

(Received July 4, 2005; revised November 4, 2005; accepted November 18, 2005; published online March 27, 2006)

A quartz tuning-fork (TF)-based scanning probe is presented for local electrical transport measurements on quantum devices below the liquid ^{4}He temperature. The TF is utilized to drive and sense the mechanical oscillation of an attached, microfabricated cantilever featuring a conductive tip made of platinum silicide. The microfabricated structure allows the application of an external voltage to the tip, while the cantilever is electrically grounded. The probe was characterized at room temperature, 70 K, and 2 K. It was found that spatial sensitivity decreased with temperature. Imaging a gold surface at 2 K was successfully performed. A number of probes can be batch-fabricated, thus shortening the lead time for conducting experiments in cryogenic scanning force microscopy. [DOI: 10.1143/JJAP.45.1992]

KEYWORDS: scanning probe microscope, atomic force microscope, quartz tuning-fork, conductive tip, microfabrication, cryogenic temperature, quantum device

1. Introduction

Local electron transport experiments on semiconductor devices can be performed using a scanning probe microscope (SPM), e.g., a conductive atomic force microscope (AFM) used as scanning gate. Such measurements are usually conducted at cryogenic temperatures in a high-vacuum environment. Under these conditions, the conventional optical readout of cantilever deflection cannot be easily implemented because of the persistent photoeffect in doped AlGaAs heterostructures. One solution is to use quartz tuning-fork (TF)-based SPM sensors,[1–6] which have several advantages in low-temperature experiments, e.g., the power dissipation is smaller than 1 nW in the standard operation mode. Applying a commercially available TF as SPM sensor requires a sharp probing tip to be mounted onto one of the prongs for imaging and probing. Various methods of implementing such a probe have been reported and summarized elsewhere.[7] We have introduced a unique realization of a TF probe, in which TFs manufactured for the watch industry (32.768 kHz) are used to drive and sense the mechanical oscillation of an attached cantilever.[7–10] The basic type[7,8] consists of a simple U-shaped microfabricated cantilever, exhibiting a sharp tip and a commercially available TF. These parts are assembled such that the two legs of the cantilever are attached symmetrically to the two prongs of the TF. The more advanced implementation[9,10] features two additional long and soft interconnecting beams for electrically contacting the tip: One end of these beams is connected to the U-shaped cantilever and the other extended end, which is shaped to form a bonding pad, is fixed on the base of the TF.

In this paper, the latest design optimized for local transport measurements on quantum devices below liquid ^{4}He temperature is introduced. The characteristics of the probe at low temperatures are described.

2. Working Principle of Probe

Figures 1(a)–1(c) show the TF probe employed in this work. The essential parts of the TF probe are the U-shaped cantilever and the TF. These pieces are used as coupled resonators. The working principle of the TF probe is the same as that of the basic type[7,8] and is summarized below.

In operation, the electrical driving signal is directly applied to the electrodes of the TF to excite vibrations at its lowest resonance. In this mode, the ends of the two prongs are moving in-plane and have opposite phases, meaning that they approach and withdraw from each other. This motion applies a small vibration at the glued ends of the cantilever; however, this vibration is in a plane perpendicular to the axis of the tip. Thus, the induced stress in the cantilever leads to an oscillating, out-of-plane motion of the tip. The amplitude of this oscillation depends on the mechanical properties of the cantilever. Compared with the vibration amplitude of the TF, an amplification can be achieved.

The TF is also used as an oscillatory force sensor similarly to a quartz microbalance. Its frequency and amplitude govern those of the tip motion, whereas the cantilever determines the spring constant and, hence, the sensitivity to the tip–sample interaction. Since a quartz TF has a much higher Q factor than a silicon cantilever of comparable resonance frequencies, the so-called frequency modulation detection,[11] which is expected to yield a higher spatial resolution than the amplitude detection, can be applied to AFM imaging under both ambient and vacuum conditions. During dynamic-mode scanning probe imaging, the resonance frequency of the TF, which differs from the eigenfrequency of the cantilever, is tracked by a phase-locked loop (PLL)[4,12,13] and kept at a set point by adjusting the tip–sample separation with a feedback loop. The amplitude of the piezoelectric current of the TF is also maintained at a set point during the operation.

3. Implementation of Probe

The first design criterion was the eigenfrequencies of the U-shaped silicon cantilever and TF in their assembled states. The resonance of the cantilever should be higher than that of the TF. The second criterion was the spring constant of the whole assembly. Here, a value of 100 N/m was required for the experiments reported in this study.

The dimensions of the cantilevers, which will meet the aforementioned criteria, were evaluated by finite element

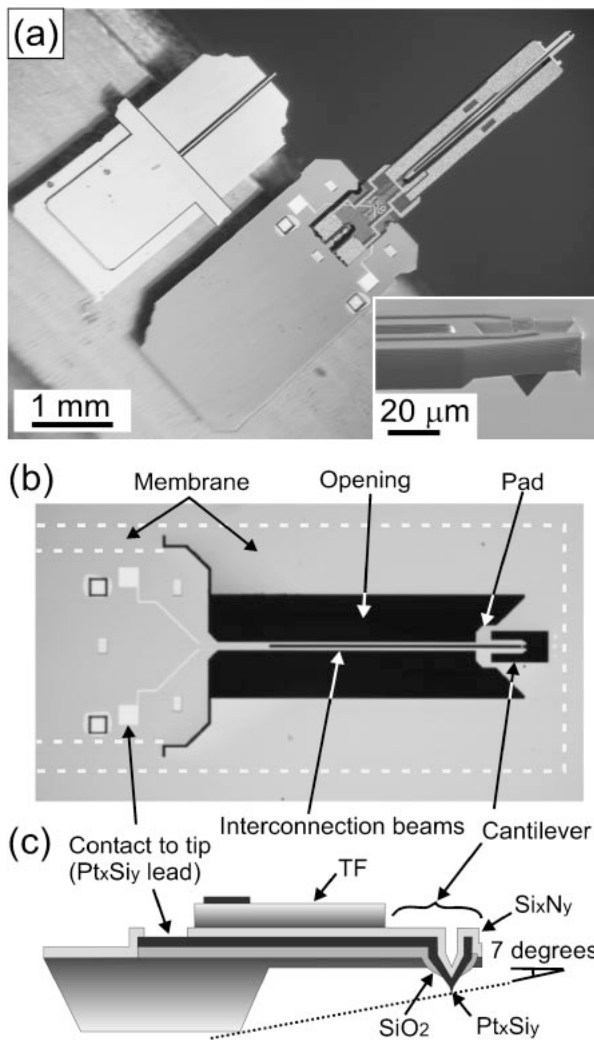

Fig. 1. (a) Top view of tuning-fork probe and standard AFM chip (upper left). The inset shows a close up view of the cantilever end. (b) Top view of cantilever chip to be assembled with tuning-fork. (c) Schematic representation of probe. The tip and the electrodes are made of platinum silicide, and are electrically isolated from the other components.

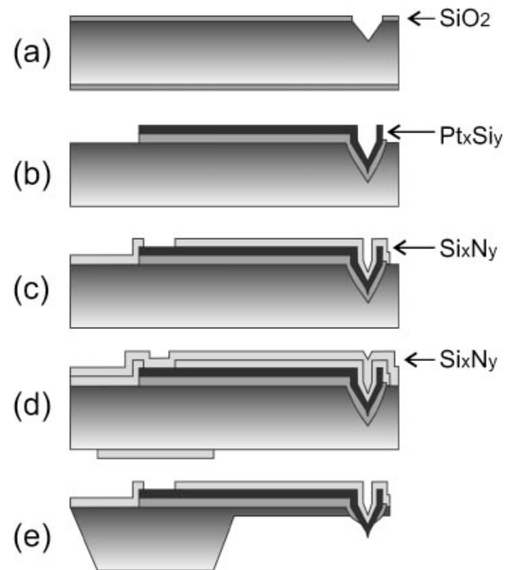

Fig. 2. Process flow chart of probe fabrication.

(FE) simulations. The other properties of the TF probe were designed to fulfill specific requirements for the application: (i) The tip had to be conductive at cryogenic temperatures, i.e., metallic and not semiconducting. Platinum silicide was chosen as tip material. It is as hard as silicon and has a conductivity comparable to that of pure platinum. In addition, it is a material compatible with microfabrication. (ii) To reduce the capacitive coupling between the conduit to the tip and the sample, the lead, which provided this contact, was electrically isolated from the cantilever and designed on its back surface. This allowed the application of an arbitrary voltage to the tip, while the cantilever itself could stay grounded. (iii) A large silicon base was designed to facilitate handling and to provide space for several contact pads. In this implementation, all silicon parts (cantilever, interconnecting beams and base) were monolithically microfabricated in a single chip. The TF was then assembled to this chip in a second step.

The key technology steps for the microfabrication were the moulding of the platinum silicide tip[14] and the fabrication of the conventional SPM beams.[15,16] The process steps are schematically presented in Fig. 2 and were as follows: First, pyramidal moulds were anisotropically etched into a silicon wafer using an oxide mask and KOH [Fig. 2(a)]. After, a so-called low-temperature oxidation of the mould to sharpen the apex, polycrystalline silicon was deposited and structured. A platinum film was deposited. Platinum silicide tips and electrodes were formed by the thermal annealing of patterned polycrystalline silicon and the deposited platinum films.[14] The oxide layer was, then, patterned by plasma etching [Fig. 2(b)]. A silicon nitride film was deposited on the entire wafer surface and patterned. A cantilever shape was patterned by reactive ion etching into silicon with a photoresist mask [Fig. 2(c)]. A second silicon nitride film was deposited on top of the electrodes and patterned to have access openings on the back side of the wafer [Fig. 2(d)]. The wafer was, then, etched in KOH to form the cantilever and chip. Finally, the second nitride film was removed and the silicide tip was exposed by removing the surrounding oxide [Fig. 2(e)]. Figure 1(b) shows a top view of the chip as fabricated. The cantilever is released and freestanding. However, the pads and the base chip are still connected to the base wafer through narrow support beams and membranes. The dotted lines in the figure indicate the area of the membrane, which will break off upon removing the chip from the wafer. The two prongs of the TF will be glued to the two pads such that the TF will cover what appears as a black opening in Fig. 1(b).

In the assembly step, TFs were glued on the chips piece by piece, using nonconductive epoxy resin (Araldite AY105/HY991). To make the probe as small as possible, we used the smallest available TF in an unpackaged version. Finally, the TF probes were separated from the base wafer by breaking the support beams and membranes.

Figure 1(a) shows a picture of the assembled probe together with a conventional SPM probe for comparison. The TF has prongs of 2.4 mm length, 130 μm thickness and 220 μm width. The beams for the interconnection are 2.0 mm long, 12 μm thick and 22 μm wide. The silicon cantilever is 350 μm long and 12 μm thick, and each leg is 49 μm wide.

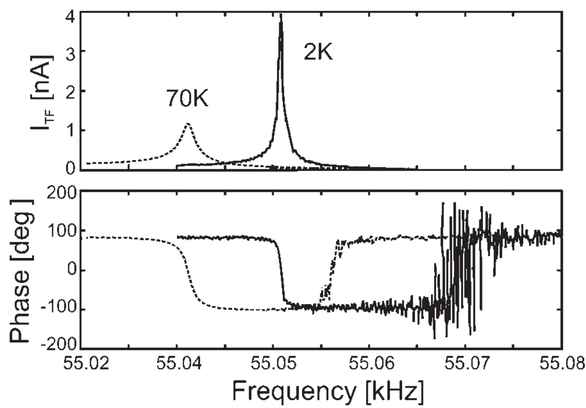

Fig. 3. Amplitude and phase of output current of TF as function of frequency in high vacuum and low temperature conditions.

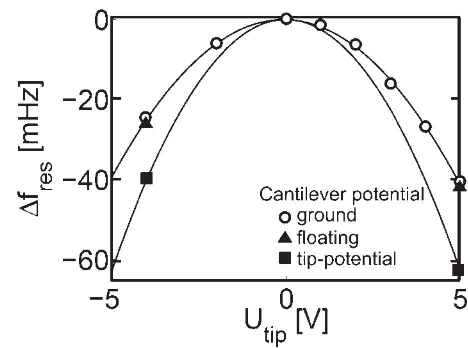

Fig. 4. Frequency shift vs applied voltage on tip under different cantilever potentials (ground, floating and at tip potential). When the cantilever was biased at the tip potential (U_{tip}), a larger electrostatic force was acting. In the other cases, the cantilever functioned as a ground-plane.

The inset in Fig. 1(a) shows a close-up view of the tip. The tip height is about 15 μm, and the typical tip radius of curvature is 20 nm. Two contact pads were designed and are shown in Figs. 1(a) and 1(b). From each pad, an interconnection of platinum silicide lead was elongated to the tip. They were electrically separated from both the silicon chip and the TF, but connected to each other at the tip. The additional pads shown in the figures were for grounding the bulk of the chip. Figure 1(c) shows a schematic representation of the probe.

4. Characterization of Probe at Low Temperature

The TF probe was mounted on an AFM platform in a ^{4}He cryostat for characterization.[4,12,13] A driving voltage of 1 mV_{rms} was directly applied to the TF, and the amplitude and phase of the output current were measured as functions of frequency under both ambient and high-vacuum conditions. The resonance frequency of the TF was 54.6 kHz at room temperature (RT) in air. Figure 3 shows the results measured at 70 K and 2 K. Both the resonance frequency and amplitude of the TF increased as temperature decreased. The mechanical quality factors were $Q = 230$ (RT, air), 2400 (RT, vacuum), 34000 (70 K, vacuum) and 96000 (2 K, vacuum). The resonance frequency of the cantilever was approximately 130 kHz at RT in air.

To evaluate the effect of the cantilever as ground plane, the tip was brought close to the surface (until a relative frequency shift of 50 mHz was observed at 2 K). Then, different dc voltages between −5 and +5 V were applied to the tip, while the gold substrate was grounded. Similarly to Kelvin probe experiments, relative frequency shift Δf_{res} was measured as a function of dc tip voltage. These experiments were conducted under three different electrical conditions of the cantilever: (i) grounded, (ii) floating, and (iii) at the dc voltage (connected to the tip). The results are shown in Fig. 4 together with fitted parabolic curves. The fact that the frequency shift is smaller when the cantilever is at a ground or floating potential shows that the capacitance between the electrical conduit at the tip and the sample was reduced using the cantilever as ground plane.

AFM imaging on a gold surface was performed at RT, 70 K, and 2 K. Figure 5 shows images taken at 2 K: a topographic image and the frequency and amplitude error signals in the PLL.[4,12,13)]

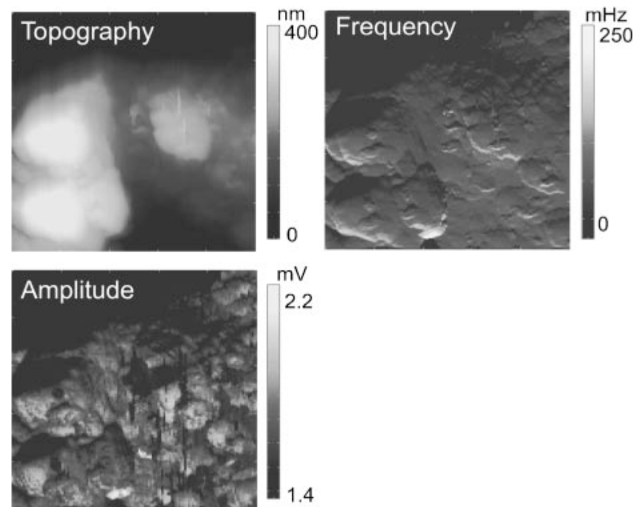

Fig. 5. Topographic image of gold surface at 2 K and simultaneously recorded frequency and amplitude error signals.

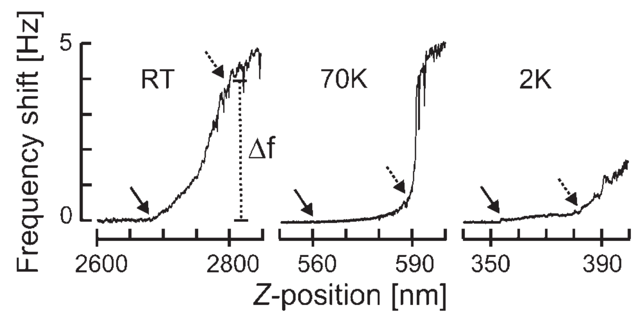

Fig. 6. Frequency shift vs tip position in *z*-direction at different temperatures. Δf indicates the total amount of frequency shift in the intermittent contact region.

Figure 6 shows the shift in the resonance frequency of the TF versus the tip position in the *z*-direction at different temperatures. The sample was again a gold film. The arrows with solid line indicate the point where the tip started tapping the sample surface and the ones with the dashed line indicate the end of this intermittent contact region (i.e., the tip remained in contact with the surface during the full oscillation cycle, whereas the cantilever was still vibrated by the TF). Beyond this second point, the probe worked in a "quasi"-contact mode.

The following characteristics were common to the special TF probe reported here as well as to ordinary probes reported earlier. The resonance frequency of the TF probe increased as the tip was pushed closer to the sample surface while in the intermittent contact region. The displacement in the z-direction, over which this region spread, was a function of the tip vibration amplitude. On the other hand, the total frequency shift in this region (denoted as Δf) was a specific and constant value for each probe, e.g., $\Delta f = 4$ Hz at RT in Fig. 6, and did not depend on tip vibration amplitude. This means that sensitivity, i.e., the frequency shift divided by the amount of tip displacement in the z-direction, differed for each setting of the tip vibration amplitude. It was further observed that probes with a lower Q-factor tended to show a higher Δf. These phenomena were detected in many experiments using different probes, operated under ambient conditions.

During the present study, we used a probe, which had characteristics similar to those of a previously used one.[10] However, the resonance frequencies of the cantilevers (72 kHz vs 130 kHz in this study) and their spring constants (66 N/m vs 100 N/m) were significantly different, and the observed Δf was approximately 20 times smaller in this study. Variations in the spring constant did not show such a marked influence on Δf in the past. Our preliminary assumption is that the much larger difference between the resonance frequency of the TF and that of the cantilever was the origin of the reduced Δf. This could be clarified by a better coupling known to exist between two oscillators, i.e., the TF and the cantilever, which have similar resonance frequencies.

5. Summary and Conclusions

A new implementation of a quartz TF-based SPM probe was presented for microscopy at cryogenic temperatures. Employing microfabrication techniques enabled us to fabricate a silicon cantilever with an electrically separated conductive tip, which was assembled to a TF used to drive and sense the mechanical oscillation of the cantilever. The successful AFM operation of the probe at RT, 70 K, and 2 K in high vacuum was demonstrated. The probe is expected to be useful for local electrical transport measurements on quantum devices below liquid ^{4}He temperature.

Acknowledgments

The authors acknowledge technical support from the staff of ComLab, the joint IMT-CSEM clean room facility. The authors thank Professor H. Shea of EPFL for having given access to his characterization laboratory. This work was financially supported by the NCCR Nanoscale Science of the Swiss National Science Foundation and the State of Neuchâtel.

1) H. Edwards, L. Taylor, W. Duncan and A. J. Melmed: J. Appl. Phys. **82** (1997) 980.
2) F. J. Giessibl: Appl. Phys. Lett. **73** (1998) 3956.
3) M. Todorovic and S. Schultz: J. Appl. Phys. **83** (1998) 6229.
4) J. Rychen, T. Ihn, P. Studerus, A. Herrmann and K. Ensslin: Rev. Sci. Instrum. **70** (1999) 2765.
5) W. H. J. Rensen, N. F. van Hulst, A. G. T. Ruiter and P. E. West: Appl. Phys. Lett. **75** (1999) 1640.
6) H. Göttlich, R. W. Stark, J. D. Pedarnig and W. M. Heckl: Rev. Sci. Instrum. **71** (2000) 3104.
7) T. Akiyama, U. Staufer and N. F. de Rooij: Rev. Sci. Instrum. **74** (2003) 112.
8) T. Akiyama, U. Staufer and N. F. de Rooij: Appl. Surf. Sci. **210** (2003) 18.
9) K. Suter, T. Akiyama, N. F. de Rooij, A. Baumgartner, T. Ihn, K. Ensslin and U. Staufer: AIP Conf. Proc. **696** (2003) 227.
10) T. Akiyama, K. Suter, N. F. de Rooij and U. Staufer: Mater. Res. Soc. Symp. Proc. **838E** (2005) O11.1.1.
11) T. R. Albrecht, P. Grütter, D. Horne and D. Rugar: J. Appl. Phys. **69** (1991) 668.
12) T. Ihn, T. Vancura, A. Baumgartner, P. Studerus and K. Ensslin: cond-mat/0112415.
13) A. Baumgartner: Ph. D. Thesis, Swiss Federal Institute of Technology Zurich, Zurich, 2005.
14) T. Akiyama, M. R. Gullo, N. F. de Rooij, A. Tonin, H.-R. Hidber, P. L. T. M. Frederix, A. Engel and U. Staufer: Jpn. J. Appl. Phys. **43** (2004) 3865.
15) O. Wolter, T. Bayer and J. Greschner: J. Vac. Sci. Technol. B **9** (1991) 1353.
16) T. R. Albrecht, S. Akamine, T. E. Carver and C. F. Quate: J. Vac. Sci. Technol. A **8** (1990) 3386.